

GENERATION OF BUBBLES USING THE RAYDROP

APPLICATION NOTE

Microbubbles were generated using the Secoya RayDrop double emulsion, a capillary based microfluidic device equipped with a 3D printed injection nozzle simplifying the generation of double emulsion when used in combination with pressure based flow controllers. We investigated how parameters such as the geometry of the nozzle and the continuous-phase flow rate affect the microbubble formation process.

CONTEXT

Microbubble generation is an area of growing interest in the microfluidic community for its potential in diverse applications (industry, life science and medicine). It has opened a new opportunity for compartmentalization of liquids/fluids for highly controlled formulations such as gas-liquid and gas-liquid-liquid emulsions. Controlled generation of bubbles in microfluidic devices generates great interests in medicine due to the ability to non-invasively image molecular events with targeted microbubbles.

Methods for robust and non-invasive imaging will be increasingly used in the future to characterize pathophysiology as well as to develop and screen new therapeutic strategies in the treatment of cardiovascular disease, cancer and inflammatory diseases for example¹. Other fields can benefit from this technology as material science^{2,3}, or to understand multiphase flows in geologic media⁴, where geometric confinement and liquid–solid physicochemical interactions play a key role.

For example, it could help to understand the way natural gas interacts with petroleum in the tiny pore spaces of underground rock formations. Bubbles can also be used to study gas-liquid physical processes such as dissolution of CO₂ in solvents, CO₂ reaction and sequestration. In this context, Mikaelian D et al. have modelled the dissolution of a chain of gas bubbles in microchannels based on mass and momentum balances⁵. Closely related to gas bubbles are foams, which are formed by trapping pockets of gas in a liquid or solid. In most foams, the volume of gas is large, with thin films of liquid or solid separating the regions of gas.

The formation of air bubbles in a liquid appears very similar to the formation of liquid or oil droplets. It begins with an elongation of the flowing material (oil, water or air), and eventually a thinning and pinch-off of the “neck” connecting the droplet or bubble to the flowing material. That pinch-off then allows the droplet or bubble to collapse into a spherical shape.

The best production mode to obtain stable and monodispersed droplets and/or bubbles follows the dripping regime, with the droplet/bubble detaching from the jet at the junction between the two immiscible phases. In the case of the RayDrop, this regime was numerically and experimentally described for production of simple emulsion of liquid droplets in Dewandre et al⁶.

In a geometry similar to the RayDrop, it has been demonstrated by Zhang et al.⁷ that in the dripping regime the bubble size decreases with the increase of the liquid flow-rate and the liquid viscosity. Bubble size is thus correlated to the capillary number $Ca = \mu u / \gamma$ with μ the viscosity of the liquid, u the speed of the liquid and γ the interfacial tension. Strong viscous forces favor the bubble breakup and decrease the bubble size, while the interfacial tension acts against the bubble breakup and increases the bubble size. Precise control of bubble size in the dripping regime is not possible with a low viscous fluid such as water at low flow rate. In this situation, the geometry of the device prevails and the bubble size is constrained by the size of channel where it is formed.

We show that with the **double emulsion** RayDrop technique, it is possible to prepare monodisperse microbubbles with a tunable size and a polydispersity index value $<1\%$. We investigated the parameters affecting the microbubble generation process, such the geometry of the nozzle and the continuous-phase flow rate. We found that the low viscous continuous phase has little impact on the bubble size formation, so when using the RayDrop single emulsion the bubble size is a function of the extraction capillary size. The geometry of the nozzle only impacts the size of the bubble while it is decoupled from the continuous-phase flow rate. The microbubble generation process using the double emulsion RayDrop technique appears more suitable to control the size and the monodispersity of microbubbles.

EXPERIMENTAL PROCEDURE

Using the double emulsion RayDrop (Secoya Technologies), controlled bubble production is achieved by dripping the core gas into a liquid coming from the shell phase, which is in turn engulfed by the third liquid, the continuous phase, as shown in Figure 1. In this case both shell and continuous phases are similar liquids. The joint action of the shell and continuous stream increases the shear stress on the very low viscosity gas stream coming from the core tip of the nozzle, and allows one to dramatically decrease the size of the bubbles. A comparison with a simple emulsion nozzle for bubble generation demonstrates the advantage of using this geometry for size control.

Fine control of the fluid flows leads to the production of bubbles with a tunable size and very low size dispersion ($CV < 0.2\%$).

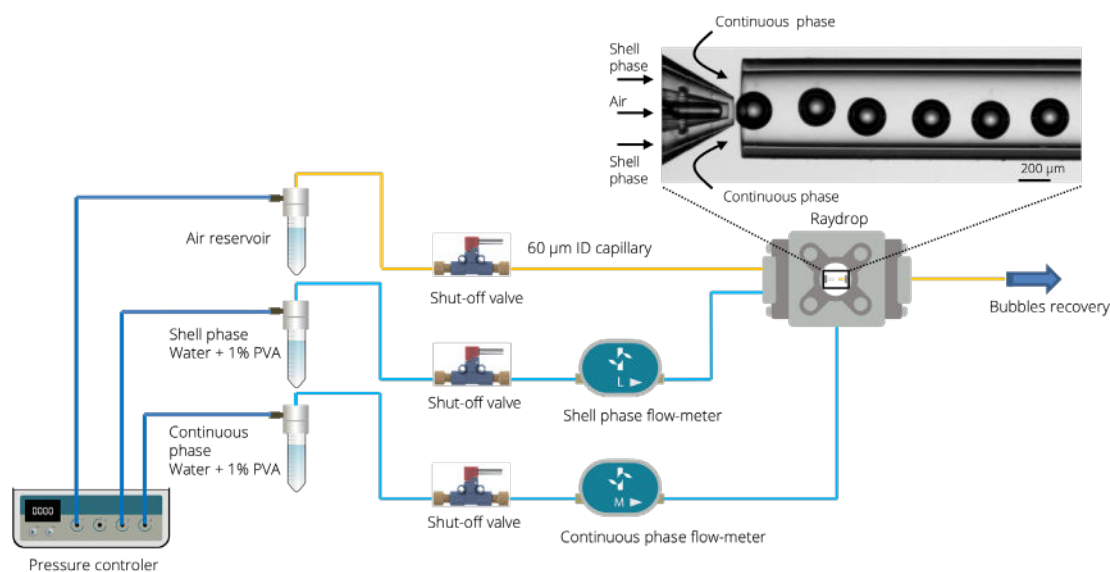


Figure 1: Scheme of the experimental setup used for the bubble generation in RayDrop.

Bubbles are formed by pumping the three fluids through the RayDrop using a pressure controller (Flow EZ, Fluigent). The flow rates of the liquids are controlled using flowmeters (Flow Unit, Fluigent). The gas flowrate is not measured but is evaluated in post-processing. As shown on the scheme in Figure 1, all reservoirs are connected to shut-off valves that can be switched off to avoid back flow. Continuous and shell phases are first pushed in the RayDrop, then when the system is stabilized, the shut-off valve of the gas is switched on.

To minimize the influence of the pressurized liquids on the compressible gas, a very high fluidic resistance is used to connect the air reservoir to the RayDrop (60 μm ID capillary, 80 cm length). A high-speed camera (MotionPro Y3, IDT) operating up to 4000 frames per second is connected to a microscope with a 10x magnification to visualize the droplets. Recorded images are then processed with ADM free software to detect the contour of the droplets, determine their size and their frequency of generation, allowing to calculate the gas flowrate.

The three different geometries used in this note are described on Figure 2. The change of geometry is easily performed by introducing two new inserts in the main chamber of the RayDrop, one with the injection nozzle and one with the output capillary.

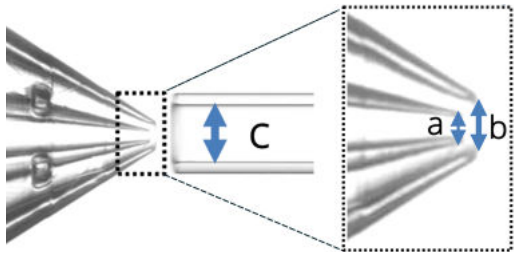
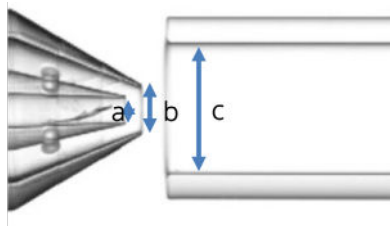
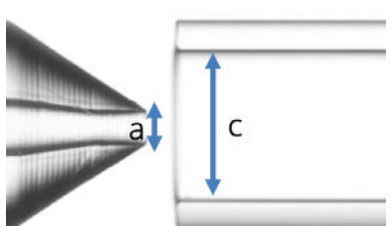
	<p>Geometry 1:</p> <ul style="list-style-type: none"> • $a=30\ \mu\text{m}$ • $b=70\ \mu\text{m}$ • $c=150\ \mu\text{m}$
	<p>Geometry 2:</p> <ul style="list-style-type: none"> • $a=90\ \mu\text{m}$ • $b=160\ \mu\text{m}$ • $c=450\ \mu\text{m}$
	<p>Geometry 3:</p> <ul style="list-style-type: none"> • $a=90\ \mu\text{m}$ • $c=450\ \mu\text{m}$

Figure 2: The three geometries used in the study

RESULT

The first experiment aims to compare the simple emulsion nozzle with the double emulsion nozzle to produce bubbles. Geometry 3 and Geometry 2 were chosen because they present the same a and c dimensions. The results are presented in Figure 3. In each case, the total water flowrate is 400 $\mu\text{L}/\text{min}$ and air flowrate $Q_{\text{air}}=120 \mu\text{L}/\text{min}$.

In a) with the Geometry 2, the total water flow-rate is divided in two parts, with the continuous phase $Q_c=300 \mu\text{L}/\text{min}$ and the shell flowrate $Q_{\text{sh}}=100 \mu\text{L}/\text{min}$ and the diameter of the bubbles is 300 μm . In b) with the Geometry 3 the equivalent diameter of the bullet shaped bubbles is 475 μm and in c) with the Geometry 2, $Q_c=400 \mu\text{L}/\text{min}$ and $Q_{\text{sh}}=0 \mu\text{L}/\text{min}$, the diameter of the bubbles is 440 μm . This clearly shows the influence of the shell stream on the size of the bubbles. It is worth to note that for each experimental point presented in the following, the coefficient of variation $CV= \text{standard deviation}/\text{mean}$, was evaluated on a minimum of 100 bubbles and was always smaller than 1%.

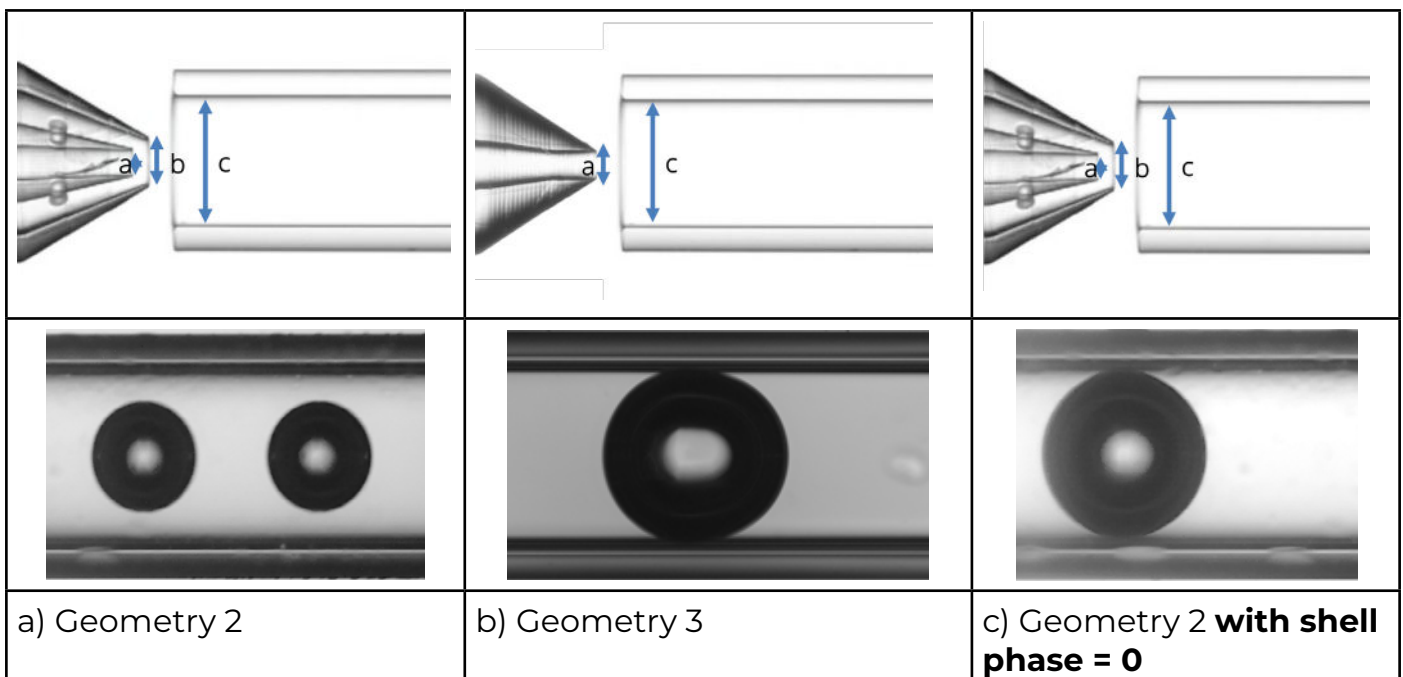


Figure 3: Comparison between Geometry 2 and 3 for a constant total water flowrate of 400 $\mu\text{L}/\text{min}$ and an air flowrate $Q_{\text{air}}=100 \mu\text{L}/\text{min}$.

Data obtained with the Geometry 3 and presented in Figure 4 further demonstrate the small influence of the continuous phase on the size of the bubble. With a single emulsion nozzle and with a low viscosity liquid, the size of the bubbles is almost totally constrained by the geometrical parameters and will be limited in the lower size to the diameter of the extraction capillary.

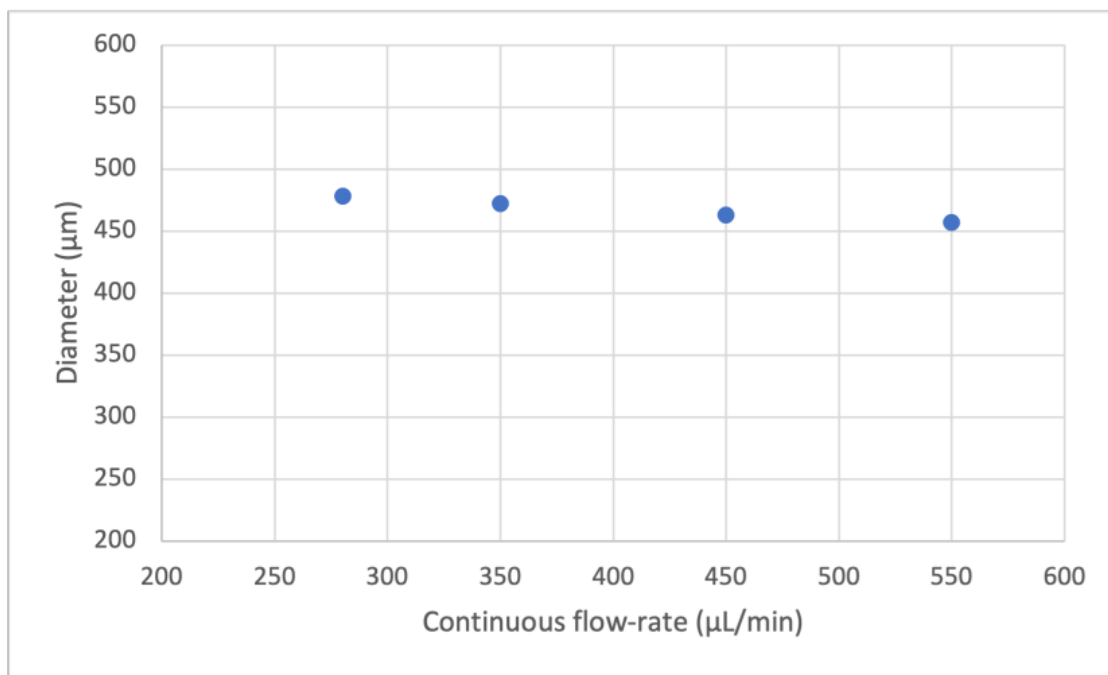


Figure 4: Bubble diameter in function of the continuous flowrate in Geometry 3. The air flowrate $Q_{air}=20 \mu\text{L}/\text{min}$. The size variation in the studied range is 4,6%.

By comparison, in the Geometry 1 and 2 with the double emulsion nozzle, the lowest size achievable is determined by both the geometrical parameters and the stream of the shell phase, as shown in Figure 5. In this case the size variation in the studied range is also equal to 5%, but the minimum size represents 61% of the extraction capillary diameter vs 99% in Geometry 2. The presence of the shell phase stream shifts the achievable size range towards lower values.

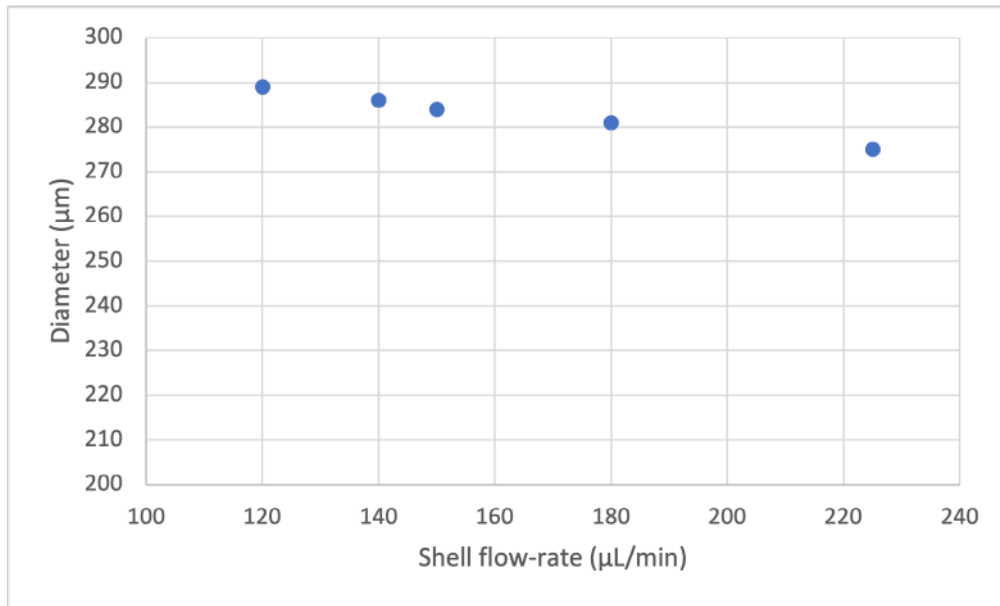


Figure 5: Bubble diameter in function of the shell flowrate in Geometry 2. The air flowrate $Q_{air}=110 \mu\text{L}/\text{min}$ and the continuous flowrate $Q_c=300 \mu\text{L}/\text{min}$. The size variation in the studied range is 5%.

The next experiment in Geometry 2, with constant shell and core flowrates shows that the increase of the continuous phase has no effect on the bubbles size in the range of the tested parameters (see Figure 6).

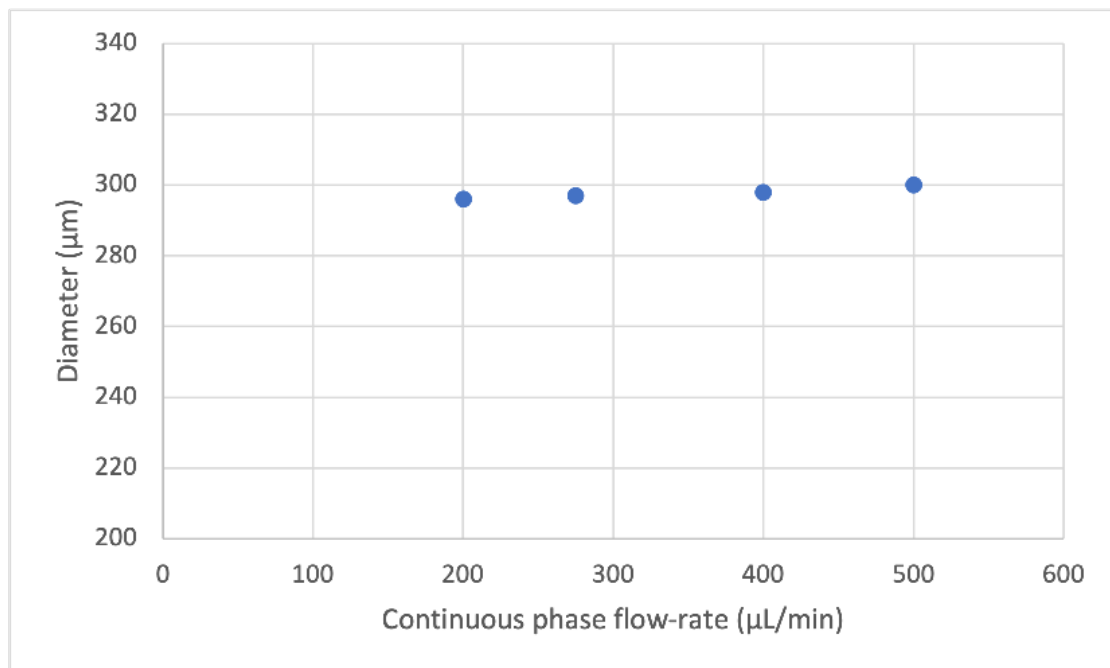


Figure 6: Bubbles diameter in function of the continuous phase flowrate. The shell flowrate $Q_{sh}=100\mu\text{L}/\text{min}$ and the air flowrate $Q_{air}=110 \mu\text{L}/\text{min}$.

Similarly, the increase of the air flowrate while keeping both water phases constant shows no influence on the bubbles size. The size, constrained by the geometrical parameters and the shell flowrate remains constant while the bubbles frequency increases with the air flowrate (see Figure 7).

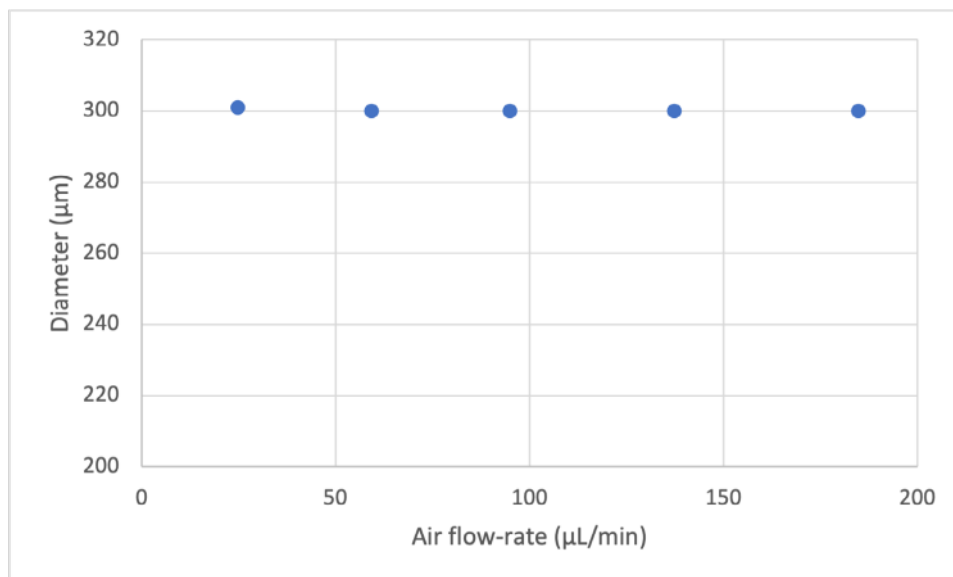


Figure 7: Bubbles diameter in function of the air flowrate in Geometry 2. The continuous phase flow-rate $Q_c=300 \mu\text{L}/\text{min}$ and the shell phase flowrate $Q_{sh}=100 \mu\text{L}/\text{min}$. The bubbles frequency increases from 29 Hz at $Q_{air}=25 \mu\text{L}/\text{min}$ to 218 Hz at $Q_{air}=185 \mu\text{L}/\text{min}$.

Similarly, with Geometry 1 bubbles smaller than the extraction capillary were obtained thanks to the presence of the shell phase. In this case the size range is from 135 to 150 µm as shown in Figure 8 where Q_c and Q_{sh} are kept constant.

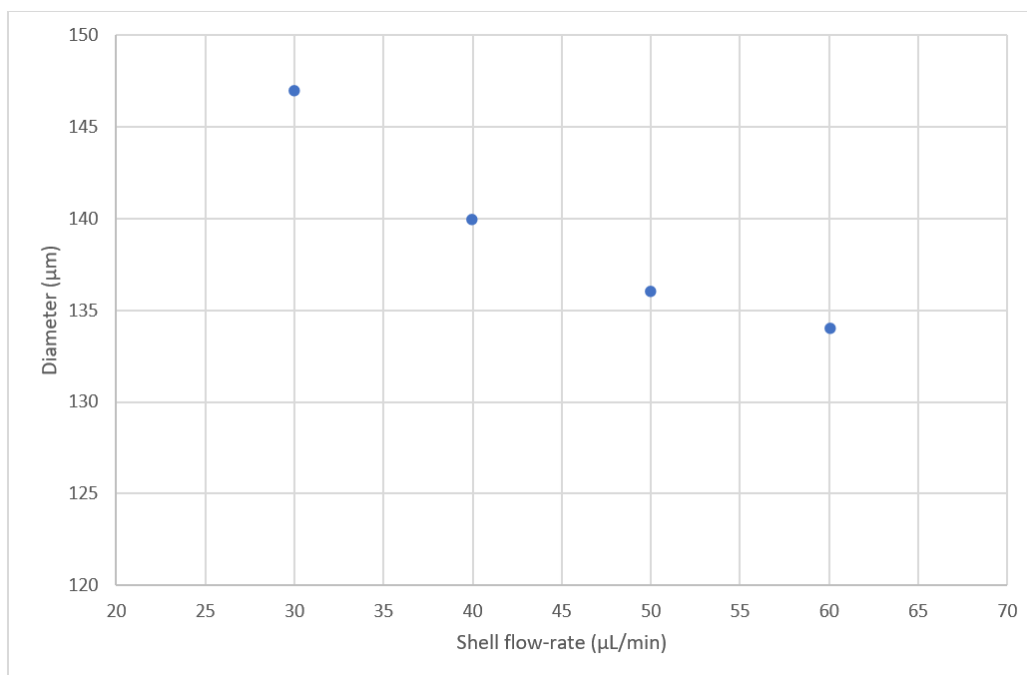


Figure 8: Bubbles diameter in function of the shell flowrate in Geometry 1. $Q_c=250 \mu\text{L}/\text{min}$ and $Q_{air}=60 \mu\text{L}/\text{min}$.

Since the geometry of the nozzle-capillary system is the most influential factor on bubble size, to optimize the system one should make the inside diameter of the capillary equivalent to the targeted bubble size. This is not feasible for bubbles smaller than 100 μm as small capillary diameter results in very high hydrodynamic resistance (proportional to the capillary radius to the power of 4), and poses pressure limitations. The solution proposed is based on the fact that local restriction of the output capillary dimension is enough to cause the confinement effect. This local restriction is obtained by using a second nozzle attached on the entry of the extraction capillary, as shown on Figure 9.

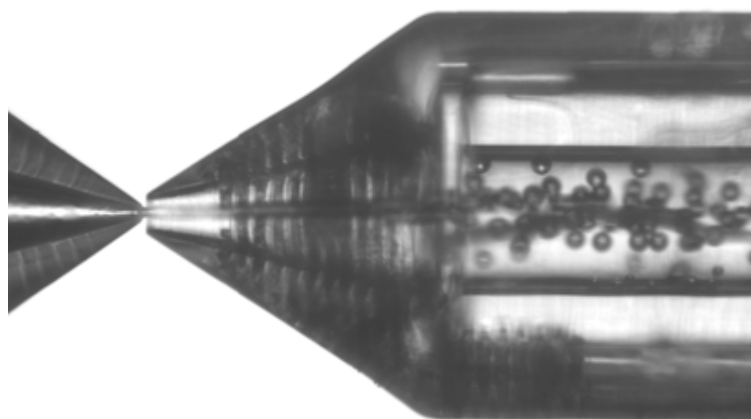


Figure 9: Nozzle with a tip inside diameter of 20 μm (left) in front of a nozzle with a tip inside diameter of 50 μm for the generation of air bubbles of 30 to 50 μm .

Using this specific geometry, the generation of air bubbles of 30 μm diameter in water at hundreds kHz is obtained in the experimental setup of Figure 1 with Fluigent pressure controller limited to 7 bar.

CONCLUSION

Microbubble generation is an area of growing interest in the microfluidic community for its potential in diverse applications (industry, life science, medicine and material science). We here show that the production of microbubbles using the double emulsion RayDrop technique is well-suited to control the size and the monodispersity of microbubbles. Of note, the geometry of the nozzle only impacts the size of the bubble while it is decoupled from the continuous-phase flow rate.

REFERENCES

1. Lindner, Jonathan R. Innovation: Microbubbles in medical imaging: current applications and future directions (2004). 3(6), 527–533. doi:10.1038/nrd1417
2. J. I. Park, A. Saffari, S. Kumar, A. Günther, E. Kumacheva, Microfluidic synthesis of polymer and inorganic particulate materials. *Annu. Rev. Mater Res.* 40, 415–443 (2010)
3. E. Amstad et al., Production of amorphous nanoparticles by supersonic spray-drying with a microfluidic nebulator. *Science* 349, 956–960 (2015)
4. Parmigiani, S. Faroughi, C. Huber, O. Bachmann, Y. Su, Bubble accumulation and its role in the evolution of magma reservoirs in the upper crust. *Nature* 532, 492–495 (2016)
5. Mikaela D, Haut B, Scheid B. Bubbly flow and gas-liquid mass transfer in square and circular microchannels for stress-free and rigid interfaces: dissolution model. *Microfluid Nanofluid* (2015) DOI 10.1007/s10404-015-1619-8
6. Dewandre, A., Rivero Rodriguez, J., Vitry, Y., Sobac, B., & Scheid, B. (2020). Microfluidic droplet generation based on non-embedded co-flow-focusing using 3D printed nozzle. *Scientific reports*, 10(1), 21616. doi:10.1038/s41598-020-77836-y
7. Zhang, J.M., Li, E.Q., Thoroddsen, S.T., 2014. A co-flow-focusing monodisperse microbubble generator. *Journal of Micromechanics and Microengineering* 24, 035008.